Cell Biol Toxicol (2025) 41:73
https://doi.org/10.1007/s10565-025-10031-9

RESEARCH

Ubiquitin-specific peptidase 10 attenuates bleomycin-induced pulmonary fibrosis via modulating autophagy depending on sirtuin 6-mediated AKT/mTOR

Shitao Mao · Na Yu · Wei Wang · Yikai Mao · Ying Du · Qihe Zhao · Xiu Gu · Jian Kang

Received: 13 August 2024 / Accepted: 16 April 2025

Abstract Idiopathic pulmonary fibrosis (IPF), characterized by fibroblast activation and collagen deposition, is a progressive lung disease that lacks effective interventions. Ubiquitin-specific peptidase 10 (USP10) acts as a multifunctional player in inflammatory response and progression of cancers, the effect on pulmonary fibrosis is unknown. Here, we demonstrated downregulated expression of USP10 in fibrotic lung tissues of IPF patients. In the current study, lung tissues were collected at the end of weeks 1, 2, or 3 post bleomycin (BLM)-intratracheal delivery. Consistently, USP10 expression levels were reduced after BLM challenge in a time-dependent manner. Mice treated with lentivirus overexpressing USP10 exhibited mitigative lung injury and reduced collagen deposition. USP10 overexpression enhanced autophagy in BLM-treated mouse lungs. Interestingly, the protective effect of USP10 was attenuated as the pulmonary autophagy flux was blocked by autophagy inhibitor 3-methyladenine (3-MA). Primary human and mouse lung fibroblasts were treated with pro-fibrotic TGF-β1 to verify the role of USP10 in vitro. Mechanically, the deubiquitinating enzyme USP10 interacted with Sirtuin 6 (Sirt6) and inhibited its degradation. Furthermore, USP10 overexpression inhibited the activation of Sirt6-mediated AKT/mTOR pathway in both lung tissues and fibroblasts. Our findings suggest that USP10 might attenuate pulmonary fibrosis through the promotion of Sirt6/AKT/mTOR-mediated autophagy. These data prioritize USP10 as a therapeutic target for treating IPF.

Keywords USP10 · Pulmonary fibrosis · Autophagy · Sirtuin 6 · AKT/mTOR promoting autophagy activity

Supplementary Information The online version contains supplementary material available at https://doi.org/10.1007/s10565-025-10031-9.

S. Mao · Y. Mao · Q. Zhao · X. Gu (✉)
Department of Pulmonary and Critical Care Medicine, The Fourth Affiliated Hospital of China Medical University, Shenyang, Liaoning, China
e-mail: xiugu@cmu.edu.cn

N. Yu · W. Wang · J. Kang (✉)
Department of Respiratory and Critical Care Medicine, The First Hospital of China Medical University, Shenyang, Liaoning, China
e-mail: kangjian58@163.com

Y. Du
Department of Otolaryngology Head and Neck Surgery, The Fourth Affiliated Hospital of China Medical University, Shenyang, Liaoning, China

Introduction

Idiopathic pulmonary fibrosis (IPF), a progressive fibrotic lung disease, characterized by fibroblast proliferation, and deposition of collagen, leading to the destruction of architecture and function (Richeldi et al.

Published online: 25 April 2025

2017; Sgalla et al. 2018). Despite efforts to explore treatment options aimed at halting or reversing the progression of IPF, available treatments are merely effective in providing short-term symptomatic relief without eradicating factors responsible for IFP (Richeldi et al. 2011, 2014). Therefore, there exists an urgent need to explore targets and develop efficacious medications for retarding the progression of IPF, and an in-depth understanding of the relevant mechanisms is a crucial task.

Autophagy, is a process of degradation of cytosolic organelles and proteins through lysosome-mediated degradation (Levine and Kroemer 2008). Autophagy is considered an adaptive response for maintaining homeostatic balance (Li et al. 2020b; Neel et al. 2013). In fact, the function of autophagy in pulmonary disease pathogenesis has been well-documented in previous research (Araya et al. 2013a; Ryter et al. 2012). Dysregulation of autophagy participates in the pathogenesis of IPF (Nakahira et al. 2016; Patel et al. 2012). In bleomycin (BLM) -induced pulmonary fibrosis, both pharmacological and genetic inhibition of autophagy processes exacerbate the fibrotic response (Singh et al. 2015). Furthermore, the loss of autophagy leads to epithelial cell senescence and myofibroblast differentiation, thus affecting IPF progression (Araya et al. 2013b; Hill et al. 2019). All these findings highlight the potential of regulating autophagy as a promising strategy for managing the progression of IPF.

To investigate the potential targets of IPF, we initially screened publicly available databases from the Gene Expression Omnibus (GEO) datasets for gene expression in IPF. Dataset GSE37635 caught our attention with multiple time points of IPF. Among the profiles identified in BLM-induced pulmonary fibrosis, ubiquitin-specific peptidase 10 (USP10) emerged as noteworthy due to its significant down-regulation, leading to further exploration of USP10 as a potential therapeutic target for IPF. USP10, a multifunctional cysteine protease, functions as an anti-stress factor and plays a regulatory role in diverse pathological and biological processes, such as viral infections and oxidative stress (Takahashi et al. 2013a, b). Notably, USP10 was found to inhibit tubular epithelial cell apoptosis and activate the NRF2/ARE pathway via Sirtuin 6 (Sirt6) (Gao et al. 2021). In addition, upregulation of USP10 can suppress myocardial fibrosis and prevent cardiomyocyte apoptosis in cases of cardiac dysfunction (Lu et al. 2021; Zhang et al. 2020). Given the well-established role of USP10 in anti-fibrosis, we here aimed to explore the role of USP10 in lung fibrotic process.

As a deubiquitinase, USP10 has shown a diverse of functions through interactions with varipus substrates (Wang et al. 2020). According to Luo's study, USP10 deubiquitinates and stabilizes its substrate Sirt6, resulting in the inhibition of hepatic steatosis and inflammation (Luo et al. 2018). Emerging evidence has confirmed that Sirt6 can alleviate IPF by suppressing epithelial-mesenchymal transition and myofibroblast differentiation (Tian et al. 2017; Zhang et al. 2019). Moreover, Sirt6 induces autophagy by modulating the autophagic flux in proteinuric kidney disease (Liu et al. 2017) and intervertebral disc degeneration (Chen et al. 2018). Consequently, it is hypothesized that the beneficial effects of USP10 overexpression in response to IPF may be attributed to its ability to induce autophagy and regulate the Sirt6-mediated AKT/mTOR pathway.

In this study, we investigated whether and how USP10 regulated pathobiology of IPF fibroblast. We first detected the expression of USP10 in IPF patients and BLM-induced mice and identified the protective effects of USP10 against IPF. In addition, human and mice fibroblasts were used to further confirm the underlying mechanisms. Mechanistically, USP10 mediated autophagy during IPF pathogenesis through the Sirt6-mediated AKT/mTOR signaling pathway. Collectively, these findings collectively indicate the involvement of autophagy and USP10 in the progression of IPF, suggesting that USP10 may serve as a promising therapeutic target for IPF.

Materials and methods

Human samples and database analysis

Lung samples from patients with IPF and normal subjects were collected. This study was approved by the Committee of the Fourth Affiliated Hospital of China Medical University. Lung samples away from the lung tumour from individuals were used as controls. Six normal and six IPF samples were used to explore USP10 expression. The transcriptome changes of IPF was determined using the GEO database (https://www.ncbi.nlm.nih.gov/geo/query/acc.cgi?acc=GSE37635), including mouse lungs at timepoint 0 as a control (n = 7); 1 (n = 7), 2 (n = 6), 3 (n = 6),

4 (n = 6) or 5 (n = 6) weeks after BLM-instillation. The R software platform was applied to analyze the data, and differentially expressed genes (DEGs) were performed using limma package. DEGs between control and BLM treatment at weeks 1–5 were identified by using a threshold of fold change ≥ 1 and adjust P value ≤ 0.05. The downregulated DEGs at each week were illustrated using the creation of heatmaps. Gene Ontology (GO) and Kyoto Encyclopedia of Genes and Genomes (KEGG) analysis were performed to annotate common downregulated genes in IPF.

Animal model of BLM-induced lung fibrosis

C57/BL6 mice (6–8 weeks) were used to conduct BLM-induced lung fibrosis. The experiments were approved by the Animal Care and Use Committee of The Fourth Affiliated Hospital of China Medical University. BLM-induced fibrosis was conducted as shown in Fig. 2A. For the establishment of the IPF model, mice were intratracheal (i.n.) instillation with bleomycin sulfate (BLM; 3 mg/kg. Macklin, B802467, China) in 50 μL saline solution. Control mice were received saline solution alone. Mice were euthanized at the point of 1w, 2w, and 3w, and lungs were harvested. The experimental mice were administered with 50 μL of lentivirus vector containing USP10 encoding fragments ($USP10^{Lv}$, 5×10^8 TU/mL) or the corresponding lentivirus particles (5×10^8 TU/mL) via i.n. injections following BLM challenge. In addition, mice were treated with the 3-methyladenine (3-MA, 30 mg/kg/day; Aladdin, 5142–23 -4, China) until the conclusion of experiment to explore the role of autophagy. The lung index was analyzed by lung weight (mg)/body weight (g).

Quantitative real-time PCR (qRT-PCR)

TRIpure buffer (BioTeke, RP1001, China) was used to extract RNA. cDNA was reversely transcribed from RNA by the PCR system. The quantification of PCR-amplification products were performed by SYBR Green system (Solarbio, SY1020, China). mRNA expression was determined by the method of $2^{-\Delta\Delta Ct}$. Primers are: mus fibronectin: 5'-CGTGCTATGACG ATGGG- 3' (F); 5'-CAGGTCTACGGCAGTTGT- 3' (R), mus collagen type I alpha1 (COL1 A1): 5'-CGC CATCAAGGTCTACTGC- 3' (F); 5'-GAATCCATC GGTCATGCTCT- 3' (R), mus USP10: 5'-CACCCG AATTTATCCTTG- 3' (F); 5'-TCTGCGTTAGAG TTGCTTT- 3' (R), and mus α-smooth muscle actin (α-SMA): 5'-GGGAGTAATGGTTGGAAT- 3' (F); 5'-TCAAACATAATCTGGGTCA- 3' (R).

Western blot analysis

Lysis buffer (Solarbio, R0010, China) containing PMSF was used to lyse lung tissues and fibroblasts. BCA Protein Assay Kits were used to calculate protein levels. Proteins were run on SDS gels, transferred to PVDF membranes. Blots were developed with primary antibodies after blockage. Antibodies used including: USP10 (ABclonal, A8748, 1:1000, China), LC3II/LC3I (ABclonal, A5618, 1:1000), p62 (ABclonal, A11250, 1:1000), AKT (Affinity, AF6261, 1:1000, China), p-AKT (Affinity, AF0016, 1:1000), COL1 A1 (ABclonal, A22090, 1:1000), Fibronectin (ABclonal, A16678, 1:1000), α-SMA (Affinity, AF1032, 1:1000), mTOR (Affinity, AF6308, 1:1000), p-mTOR (Affinity, AF3308, 1:1000), Sirt6 (ABclonal, A18468, 1:1000). After incubation with second antibodies for 1 h, bands were developed with ECL solution and analyzed using Gel-Pro-Analyzer.

Immunofluorescence (IF) staining

Paraffin-embedded samples were deparaffinised, blocked with 1% BSA, and incubated with USP10 (1:50, Santa cruz, sc- 365828, China) combined with anti-Sirt6 primary antibody (1:50, Proteintech, 13,572–1-AP, USA) or anti-Vimentin (1:50, ABclonal, A19607). The sections were then incubated with a mixture of secondary antibodies (FITC-conjugated and Cy3-labeled antibodies) for 90 min at 37 °C. The fixed fibroblasts were cultured with Triton X-100 and blocked. After being incubated with primary antibodies against α-SMA (1:50, ABclonal, A17910) and Vimentin (1:50, ABclonal, A19607), cells were developed with Cy3-labeled goat anti-rabbit IgG (1:200). The sections were incubated with USP10 (1:50, Santa cruz, sc- 365828) combined with anti-Sirt6 primary antibody (1:50, Proteintech, 13572–1-AP) and developed with Cy3-labeled goat anti-mouse IgG or FITC-labelled goat anti-rabbit IgG. Slides were stained with DAPI. Following sealed tablets with anti-fluorescence quenching agents, images were acquired with a fluorescent microscope (Olympus).

Histological examination

The lung samples were embedded and sectioned at 5-μm for histological analysis. Hematoxylin and eosin (H&E) staining was performed to visualize the inflammatory status and morphological changes of the tissues. Masson staining was prepared to determine the collagen content and distribution using an optical microscope (Olympus). In addition, autophagy in the mice lung tissues and fibroblasts was characterized by transmission electron microscopy (TEM) microscopy (H- 7650, Hitachi, Japan).

Immunohistochemistry analysis (IHC)

IHC staining was used to determine the expression of α-SMA. The fixed sections were blocked with non-specific antigen and cultured with an anti-α-SMA antibody (1:50; ABclonal, A17910) overnight at 4 °C. After being incubated with HRP-labeled secondary antibody (1:500), slides were developed with DAB. Following counterstain, representative stained pictures were captured under a microscope (Olympus).

Primary lung fibroblasts culture

Primary human lung fibroblasts (HLF) from lung samples were derived from consenting donors (n = 3) and isolated as previously described (Li et al. 2020a). Briefly, lungs were mechanical dispersal and incubated with 1 mg/mL collagenase IV for 1–2 h. Cells were harvested by centrifugation and redispersed in DMEM containing 10% FBS, 100 μg/mL streptomycin, and 50 μg/mL penicillin. Early passages were used, and fibroblasts were incubated with Vimentin (Fig. S1A). Primary mouse lung fibroblasts (MLF) were obtained from iCell (MIC-iCell-a010, China) and cultured in the primary fibroblast culture system (iCell; PriMed-iCell- 003) at 37 °C. Fibroblasts were incubated with Vimentin (Fig. 6A).

Fibroblasts were treated with 10 ng/mL mouse recombinant TGF-β1 (Sino Biological, 80,116-RNAH, China) for 24 h to induce fibroblast activation. Lentivirus containing USP10 encoding fragments ($USP10^{Lv}$) and empty vector (Vector) were constructed and infected fibroblasts for 48 h. Fibroblasts were harvested and treated with TGF-β1 and/or 3-MA (2 mM) for another 24 h and collected for assays.

Statistics analysis

GraphPad software was used to analyze obtained data. $P < 0.05$ was considered statistically significant. All data were expressed as mean ± SD. Differences among groups were 151 analyzed by Student's t test and one-way analysis of variance.

Results

Identification of DEGs in BLM-injured mice

We first determined transcriptome changes of IPF based on GSE37635 datasets (Blaauboer et al. 2013). This dataset encompassed analysis of lung tissues from control and mice with 1–5 weeks BLM treatment. Expression of DEGs at different time points of IPF was compared with control as shown in Fig. S2A. Notably, a significant difference in gene expression was observed at 1-week post-BLM treatment, with a gradual decrease in the number of DEGs in subsequent weeks, and there were only 3 DEGs at week 5 post-BLM. Subsequently, GO and KEGG analyses elucidated the functional process associated with DEGs at week 3 post-BLM treatment. DEGs were predominantly centered on inflammation and immune response, encompassing functions such as response to chemokine and regulation of autophagy (Fig. S2B; right panel). Furthermore, the enriched KEGG pathways at week 3 were predominantly associated with cytokine-cytokine receptor interaction and the AKT/mTOR signaling pathway (Fig. S2B; left panel). Attention was directed towards the downregulated DEGs and the expression of DEGs annotated in Fig. S2C. These selected DEGs were associated with signal transduction pathways, such as NF-kappaB signaling pathway, regulation of autophagy, and cellular response to interleukin- 1 (Fig. S2D). USP10 was selected as a potential target for IPF, and we further determined the impact of USP10 on the progression of IPF.

USP10 is downregulated in the lungs of IPF patients and BLM-injured mice

We first detected USP10 expression in healthy and IPF lungs, and the results showed that USP10 was downregulated in human lungs of IPF patients (Fig. 1A). We checked tissues from IPF patients by co-immunostaining

of USP10 and Vimentin, a fibroblast marker, and interestingly found that USP10 was co-expressed with Vimentin (Fig. 1B). As shown in Fig. 2B, the expression value of USP10 was decreased in lung tissues after 1, 2, and 3 weeks of BLM treatment in the public dataset. BLM-induced pulmonary fibrosis in mice was conducted. Consistently, USP10 expression was gradually decreased following BLM treatment for 1, 2, and 3 weeks (Fig. 2C). A significant increase in Vimentin was observed in response to BLM treatment, confirming the presence of fibrosis. Notably, alongside the upregulation of Vimentin, the expression of USP10 was downregulated and colocalized with Vimentin (Fig. 2D).

USP10 relieves BLM-induced lung injury

Given the observed decrease of USP10 in IPF patients and mice, the biological significance of USP10 was determined. Mice with USP10 overexpression were generated following BLM treatment and then administrated with autophagy inhibitor 3-MA. As expected, USP10 was increased in USP10 vector-injected mice, and 3-MA treatment did not impact the expression of USP10 (Fig. 3A). BLM treatment increased the lung index, and USP10 overexpressed mice exhibited a reduced lung index value after BLM treatment for 3 weeks (Fig. 3B). The lung sections from BLM-treated mice showed increased alveolar septal thickening, excess collagen, and fibrosis lesions, as demonstrated by histological assessments (Fig. 3C, D). Importantly, the fibrotic lesions were markedly suppressed with USP10 overexpression. The protective effect of USP10 overexpression was reversed by the autophagy inhibitor 3-MA.

USP10 promotes autophagy and attenuates lung fibrosis in BLM-induced lungs

The expression of α-SMA was remarkably upregulated in BLM-treated mice (Fig. 4A). Immunofluorescence staining of tissues in USP10 overexpressed mice showed that USP10 expression was increased

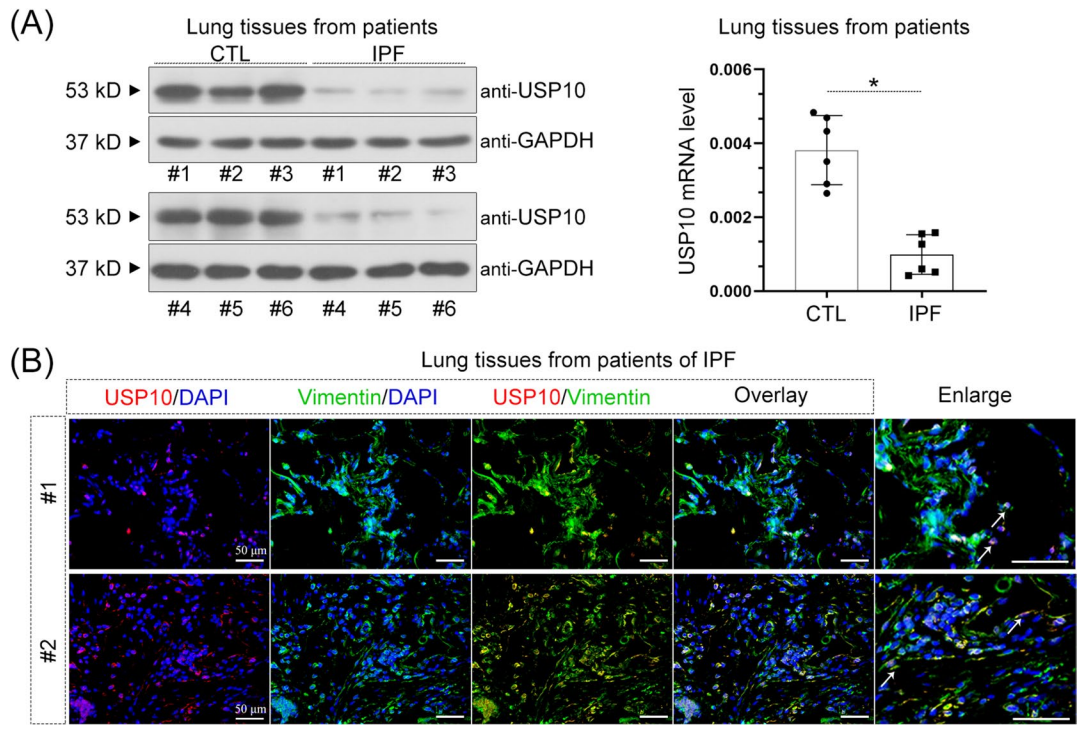

Fig. 1 USP10 is downregulated in the lungs of IPF patients. **(A)** Western blot and Real-time PCR of USP10 in lungs from IPF patients and healthy individuals showed that USP10 expression was downregulated. Each bar represents the mean ± SD; $^{*}p < 0.05$ vs. CTL group. **(B)** Representative images of double-labeled immunofluorescence staining of USP10 (red) and Vimentin (green) in the lung sections from patients with IPF. Blue indicates nucleus marked with DAPI. USP10, ubiquitin-specific peptidase 10; IPF, idiopathic pulmonary fibrosis; CTL, control

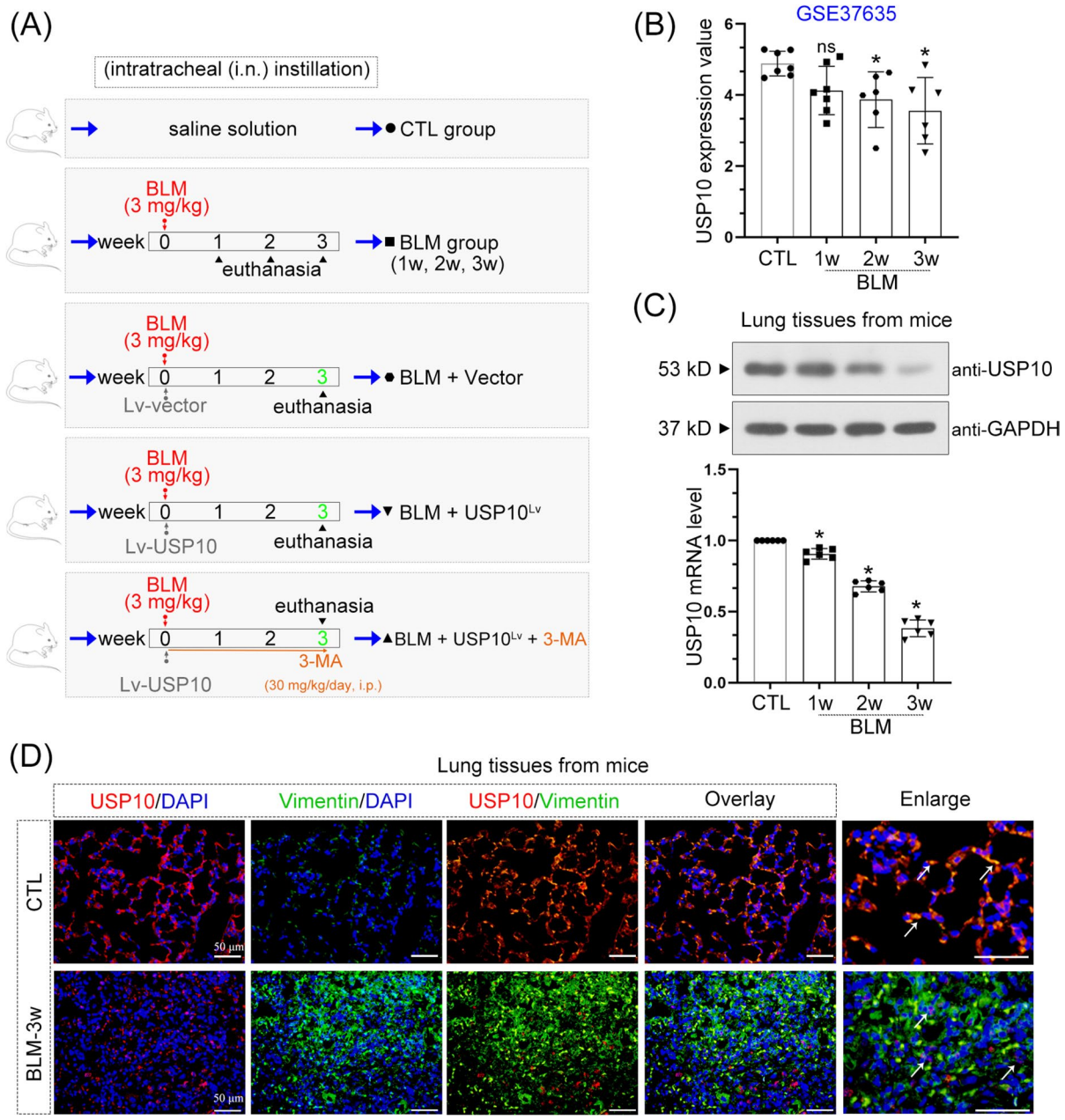

Fig. 2 USP10 expression is decreased in the lungs from BLM-induced mice. **(A)** Schematic chart showing the induction of BLM-induced IPF and experiment protocol. **(B)** USP10 expression values in GSE37635 datasets (https://www.ncbi.nlm.nih.gov/geo/query/acc.cgi?acc=GSE37635) based on the GEO database (https://www.ncbi.nlm.nih.gov/geo/geo2r/) showed that USP10 expression was downregulated in BLM-induced mice lung tissues at the indicated times. Each bar represents the mean ± SD; $^{*}p < 0.05$ vs. CTL group. **(C)** Western blot and Real-time PCR of USP10 in lungs from BLM-treated mice showed that USP10 expression was downregulated in lung tissues at the indicated times. Each bar represents the mean ± SD; $^{*}p < 0.05$ vs. CTL group. **(D)** Representative images of double-labeled immunofluorescence staining of USP10 (red) and Vimentin (green) in pulmonary tissues. Blue indicates nucleus marked with DAPI. USP10, ubiquitin-specific peptidase 10; BLM, bleomycin; IPF, idiopathic pulmonary fibrosis; GEO, Gene Expression Omnibus; CTL, control

in fibroblasts, as demonstrated by colocated with Vimentin (Fig. 4B). Accordingly, the fibrotic-related proteins, COL1 A1, fibronectin, and α-SMA, were largely preserved in the lungs of BLM-induced mice, but there was a reduction in these levels with US910 overexpression (Fig. 4C). Notably, the aforementioned alterations were reversed following treatment with 3-MA.

Given that autophagy inhibitor abrogated the role of USP10 in fibrosis, we inferred that USP10

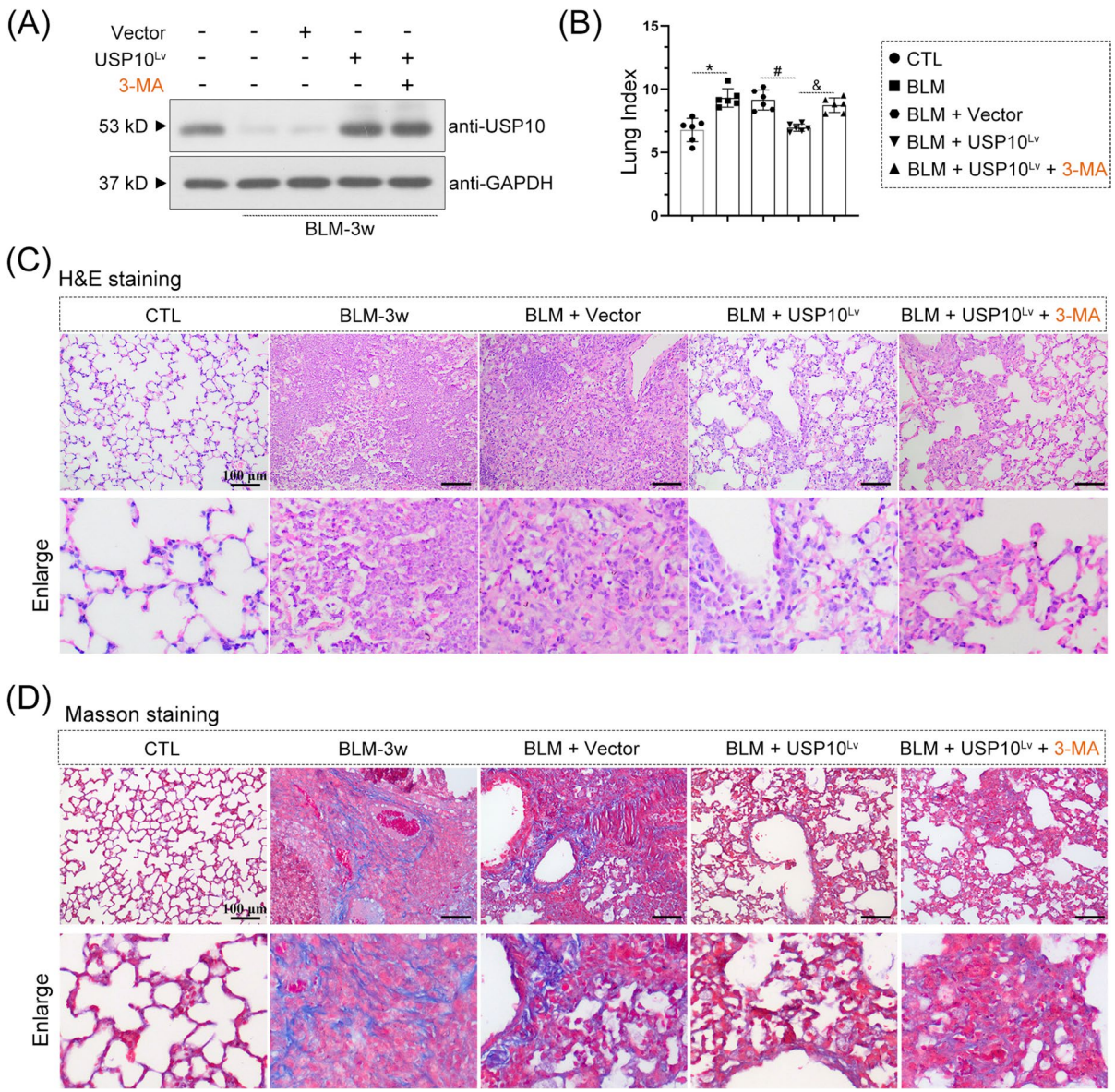

Fig. 3 USP10 overexpression ameliorates the symptoms of pulmonary fibrosis in BLM-induced mice. **(A)** Western blot results confirmed that overexpressed USP10 in the lung tissues, indicating that the lentivirus vector was constructed successfully. **(B)** Effect of USP10 on lung index of BLM-induced mice. $^{*}p < 0.05$ vs. CTL, $^{\#}p < 0.05$ vs. BLM + Vector group, $^{\&}p < 0.05$ vs. BLM + USP10^{Lv} group. **(C, D)** H&E and Masson images indicated that the alveolar wall became thicker and excess collagen was deposited in lung tissues from BLM-treated mice. USP10 overexpression alleviated collagen deposition, and 3-MA treatment aggregated these symptoms. USP10, ubiquitin-specific peptidase 10; BLM, bleomycin; IPF, idiopathic pulmonary fibrosis; CTL, control. Lv, lentiviral vector

might affect autophagy activity in IPF. We investigated the expression of autophagy-related marker proteins, including LC3II (autophagosome marker) and p62 (a degradation substrate of autophagy). As indicated in Fig. 4D, LC3II/LC3I level was increased and p62 expression was decreased in BLM-induced lung tissues. USP10 overexpression further increased the LC3II/LC3I ratio and suppressed p62 expression, suggesting that USP10 activated autophagy. To confirm the activation of autophagy, TEM was performed to investigate the formation of lysosomes in BLM-induced lungs. As shown in Fig. 4E, overexpressed USP10 activated autophagy by promoting lysosome formation.

USP10 interacts with Sirt6 and mediates Sirt6-related AKT/mTOR signaling pathway

In lung tissues with IPF, the levels of USP10-targeted gene Sirt6 were found to be increased. Moreover, USP10 was found to co-express with Sirt6, as illustrated in Fig. 5A. Sirt6 expression was further confirmed by Western blot assay (Fig. 5B). The activation of Sirt6-related AKT/mTOR signaling was examined, and AKT/mTOR pathway was activated by BLM treatment, evidenced by increased phosphorylation of AKT and mTOR without changing the level of total AKT and mTOR (Fig. 5B). Interestingly, USP10-overexpressed mice exhibited decreased expression levels of p-AKT and p-mTOR. Collectively, these results indicate that pulmonary USP10 overexpression alleviates the activation of the Sirt6-mediated AKT/mTOR signaling pathway.

USP10 inhibits TGF-β1-induced fibrogenesis in MLF

After treatment with TGF-β1, USP10 expression was examined in MLF, revealing a downregulation of USP10 (Fig. 6B, C). The lentivirus vector consisting of USP10 or empty vector was conducted and infected fibroblasts to investigate USP10 function. TGF-β1 challenge reduced a notable decrease in USP10 expression in MLF, while its expression increased after USP10 overexpression (Fig. 6E). Immunofluorescence staining showed that the expression of α-SMA was significantly upregulated following TGF-β1 treatment, and USP10 inhibited TGF-β1-induced α-SMA expression (Fig. 6D). Cultured MLF with TGF-β1 resulted in a rapid elevation in fibrotic markers. USP10 induction blocked the induction of these factors (Fig. 6F). In light of these findings, it can be inferred that USP10 functions as an anti-fibrotic factor capable of thwarting pulmonary fibrosis.

USP10 promotes autophagy and attenuates fibrosis in MLF

Upon treatment with TGF-β1, the level of LC3II/LC3I was significantly decreased, and p62 was increased notably. Conversely, USP10 overexpression promoted autophagy activity (Fig. 7A). To delve deeper into autophagic response, TEM was employed and the results revealed that only empty single-layer vacuoles were noted in the TGF-β1-treated fibroblasts, and double-membrane structures containing organelle components, characteristics of autophagosomes, were identified in USP10-treated fibroblasts (Fig. 7B). Furthermore, our observations revealed the activation of the AKT/mTOR signaling pathway following pre-treatment with TGF-β1. Interestingly, USP10 overexpression demonstrated the capability to decrease levels of p-mTOR and p-AKT, thereby sustaining autophagic activity (Fig. 7C, D).

We then evaluated the fibrotic indicators in TGF-β1/3-MA-treated MLF. As indicated in Fig. 7E,

Fig. 4 USP10 overexpression promotes autophagy induction in BLM-induced lung tissues. **(A)** Immumohistochemical staining showing that α-SMA was highly expressed in BLM-treated mouse lung slices, USP10 overexpression decreased α-SMA expression. **(B)** Representative images of double-labeled immunofluorescence staining of USP10 (red) and Vimentin (green) in mouse lung tissues in different groups. Blue indicates nucleus marked with DAPI. **(C)** Fibrotic proteins including COL1 A, fibronectin, and α-SMA increased in the BLM-treated mice. USP10 overexpression reversed fibrotic protein expression. **(D)** BLM treatment resulted in marked upregulation of LC3II and downregulation of p62 protein levels. USP10 overexpression reversed the marker of autophagosome expression. **(E)** Representative images of autophagosomes examined using a TEM analysis in mouse lung slices. Scale bar = 1μm. USP10, ubiquitin-specific peptidase 10; BLM, bleomycin; α-SMA, α-smooth muscle actin; COL1 A, collagen type I alpha1; TEM, transmission electron microscope ▶

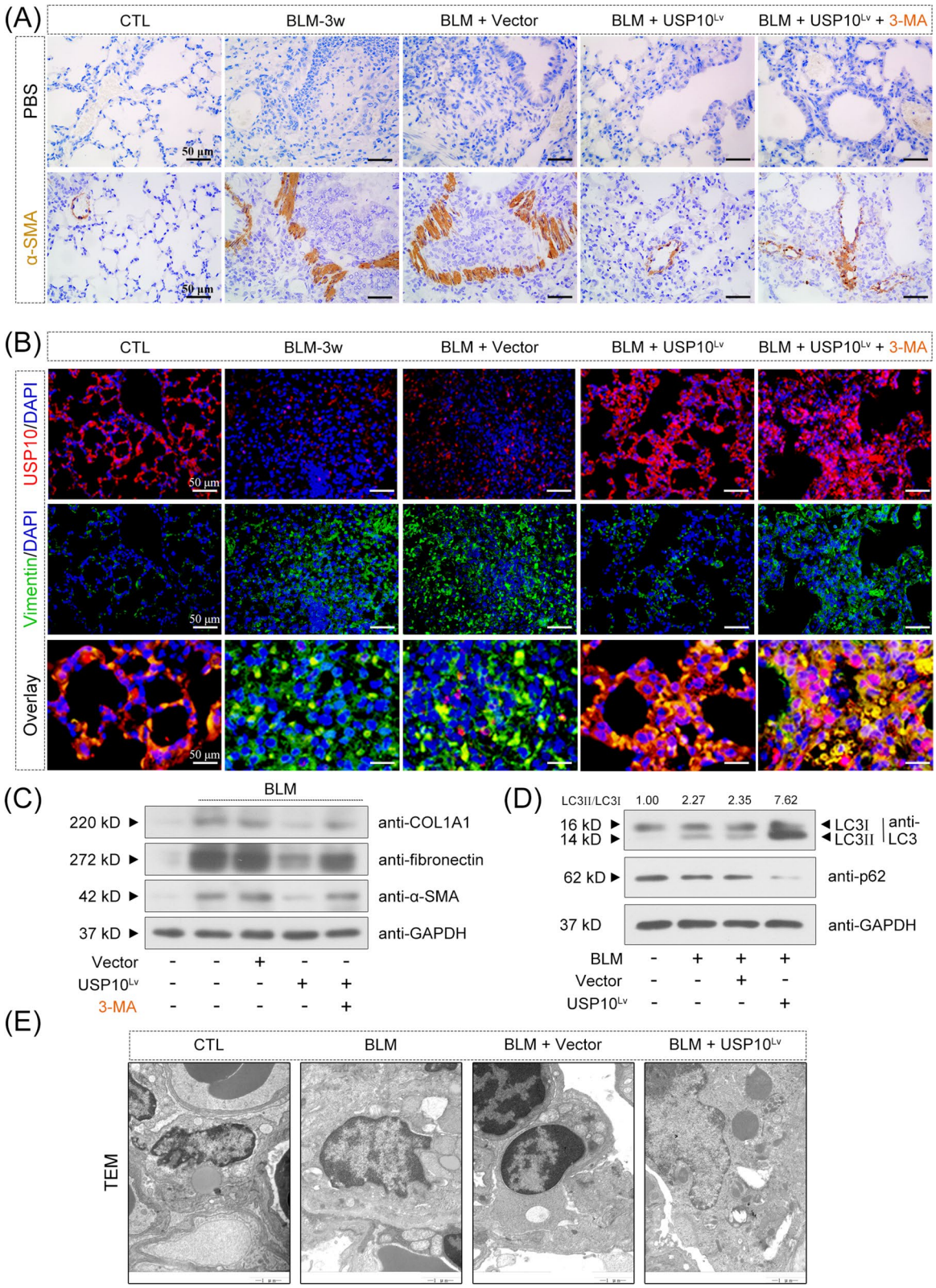
(A)
CTL
BLM-3w
BLM + Vector
BLM + USP10Lv
BLM + USP10Lv + 3-MA
PBS
α-SMA
50 μm
(B)
USP10/DAPI
Vimentin/DAPI
Overlay
(C)
BLM
220 kD
272 kD
42 kD
37 kD
anti-COL1A1
anti-fibronectin
anti-α-SMA
anti-GAPDH
Vector
USP10Lv
3-MA
(D)
LC3II/LC3I
1.00
2.27
2.35
7.62
16 kD
14 kD
LC3I
LC3II
anti-LC3
62 kD
anti-p62
anti-GAPDH
BLM
Vector
USP10Lv
(E)
TEM

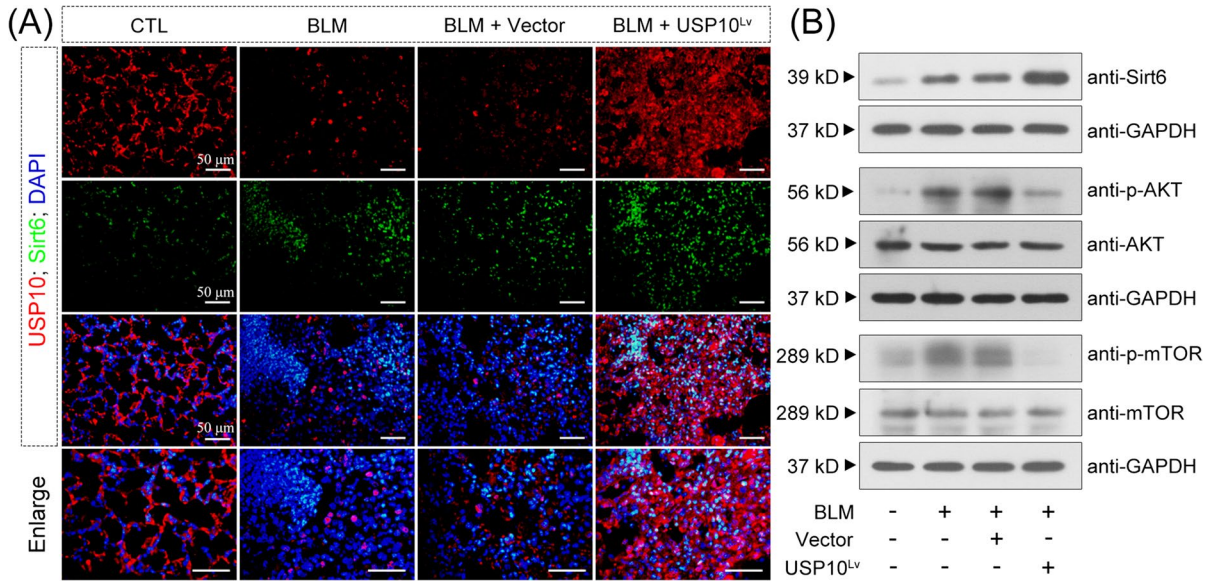

Fig. 5 Effect of USP10 on Sirt6-mediated AKT/mTOR signaling pathway. **(A)** Representative images of double-labeled immunofluorescence staining of USP10 (red) and Sirt6 (green) in pulmonary tissues. Blue indicates nucleus marked with DAPI. **(B)** Western blot results exhibited that Sirt6, p-AKT, and p-mTOR were highly upregulated by BLM treatment. USP10 overexpression inhibited the expression of p-AKT and p-mTOR. USP10, ubiquitin-specific peptidase 10; Sirt6, Sirtuin 6; BLM, bleomycin

the decreased levels of COL1 A1, fibronectin, and α-SMA in fibroblasts transfected with USP10 were reversed upon 3-MA treatment. Immunofluorescence staining of lung fibroblasts further revealed that the expression of α-SMA was markedly reduced following USP10 overexpression and was enhanced in fibroblasts treated with 3-MA (Fig. 7F).

Knockdown of Sirt6 abrogates USP10 overexpression-mediated effects

We inferred that USP10 exerted function in IPF through the regulation of Sirt6. Hence, the expression of USP10 and Sirt6 was detected in MLF. Results of immunofluorescence represented the co-localization of USP10 and Sirt6 fluorescence as shown in Fig. 8A. Moreover, gain-function studies revealed that USP10 overexpression led to an increase in Sirt6 protein level (Fig. 8B). The stability of Sirt6 protein was measured by using cycloheximide (CHX), and the results indicated that Sirt6 stability was enhanced by USP10 overexpression (Fig. 8C).

MLF were co-infected with lentivirus carrying shSirt6 and USP10 vector. Sirt6 expression was increased by USP10 overexpression, however, this effect was counteracted by interference with Sirt6 (Fig. 8D). The rescue experiment elucidated that interference on Sirt6 expression reversed the augmenting impact of USP10 overexpression on autophagic proteins LC3-II/LC3-I (Fig. 8E). Interference of Sirt6 expression mitigated the reduction in levels of p-AKT and p-mTOR in fibroblasts overexpressing USP10 (Fig. 8F, G). Thus, these data suggested that the effect of USP10 on fibrosis depends on Sirt6.

USP10 inhibits TGF-β1-induced fibrogenesis in HLF

We further determine whether USP10 affected IPF in TGF-β1-induced HLF. Consistent with MLF, USP10 was decreased after treatment with TGF-β1 and increased in USP10-overexpressed HLF (Fig. S1B, C). Fibrotic markers were increased in TGF-β1-treated fibroblasts and reduced after induction of USP10 (Fig. S1D). Furthermore, the promotion impact of USP10 on autophagy response was

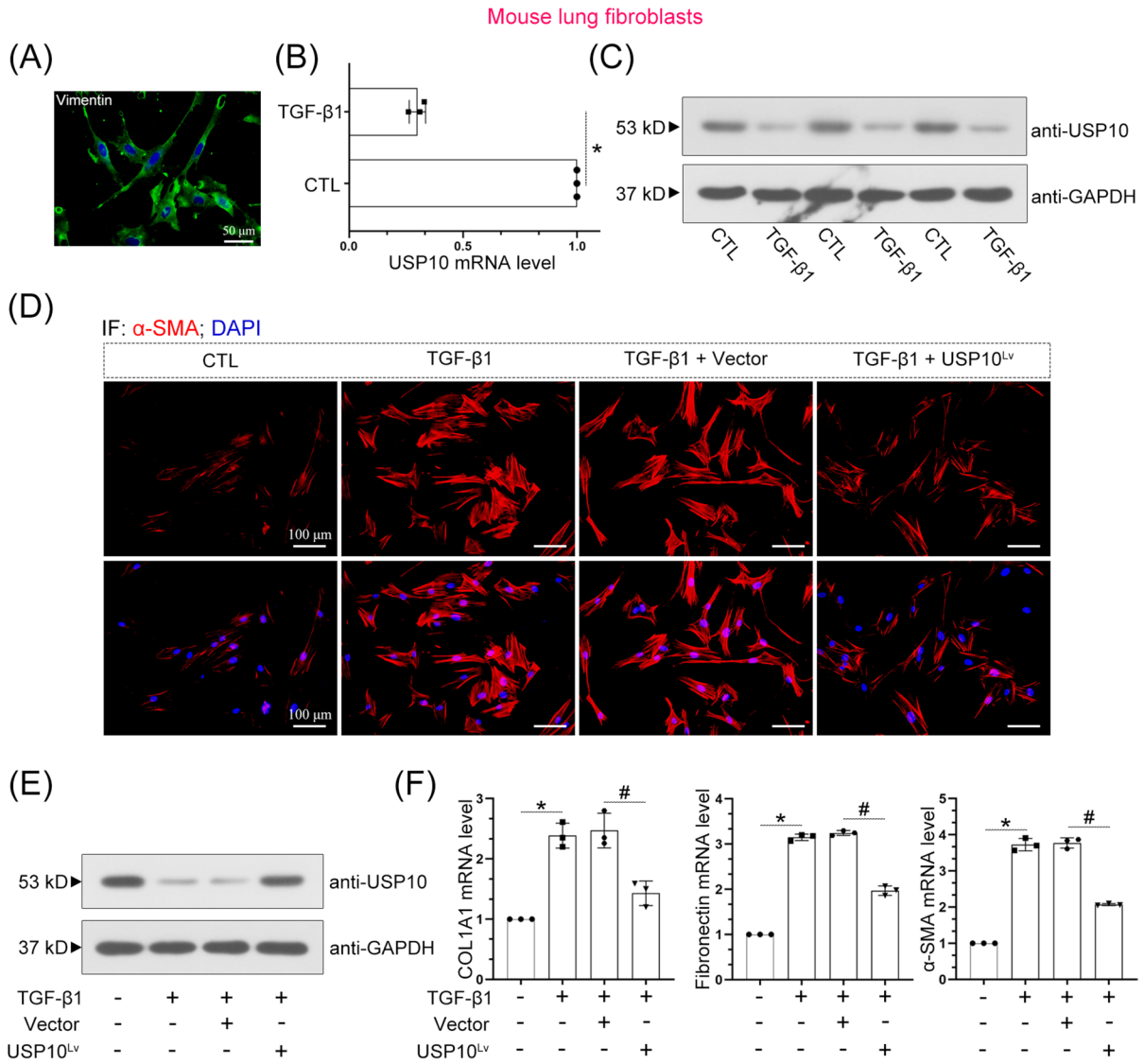

Fig. 6 Anti-fibrotic function of USP10 in mouse lung fibroblasts. **(A)** Identification of mouse lung fibroblasts; the cells were observed to display fusiform. **(B)** Real-time PCR of USP10 showing that USP10 was decreased in MLF after treatment with TGF-β1. Each bar represents the mean ± SD; $^{*}p < 0.05$ vs. CTL group. **(C)** Western blot of USP10 in MLF after TGF-β1 treatment. **(D)** Immunofluorescence staining of α-SMA in the TGF-β1-treated fibroblasts. α-SMA expression was increased after TGF-β1 treatment and decreased by USP10 overexpression. Blue indicates nucleus marked with DAPI. **(E)** Western blot results indicated that USP10 was downregulated by TGF-β1 treatment and reversed after overexpression of USP10. **(F)** Real-time PCR results exhibited that COL1 A, fibronectin, and α-SMA were highly upregulated by TGF-β1 treatment. USP10 overexpression inhibited the expression of COL1 A, fibronectin, and α-SMA. Each bar represents the mean ± SD; $^{*}p < 0.05$ vs. CTL group; $^{\#}p < 0.05$ vs. TGF-β1 + Vector group. USP10, ubiquitin-specific peptidase 10; α-SMA, α-smooth muscle actin; COL1 A, collagen type I alpha1. MLF, mouse lung fibroblasts

demonstrated In HLF, as indicated by increased levels of LC3II/LC3I and decreased p62 (Fig. S1E). The activation of the AKT/mTOR pathway was confirmed in TGF-β1-induced HLF, and USP10 overexpression inhibited AKT/mTOR activation (Fig. S1F, G). The interaction between USP10 and Sirt6 was further detected in HLF. Likewise, USP10 was co-expressed with Sirt6 (Fig. S1H), and USP10

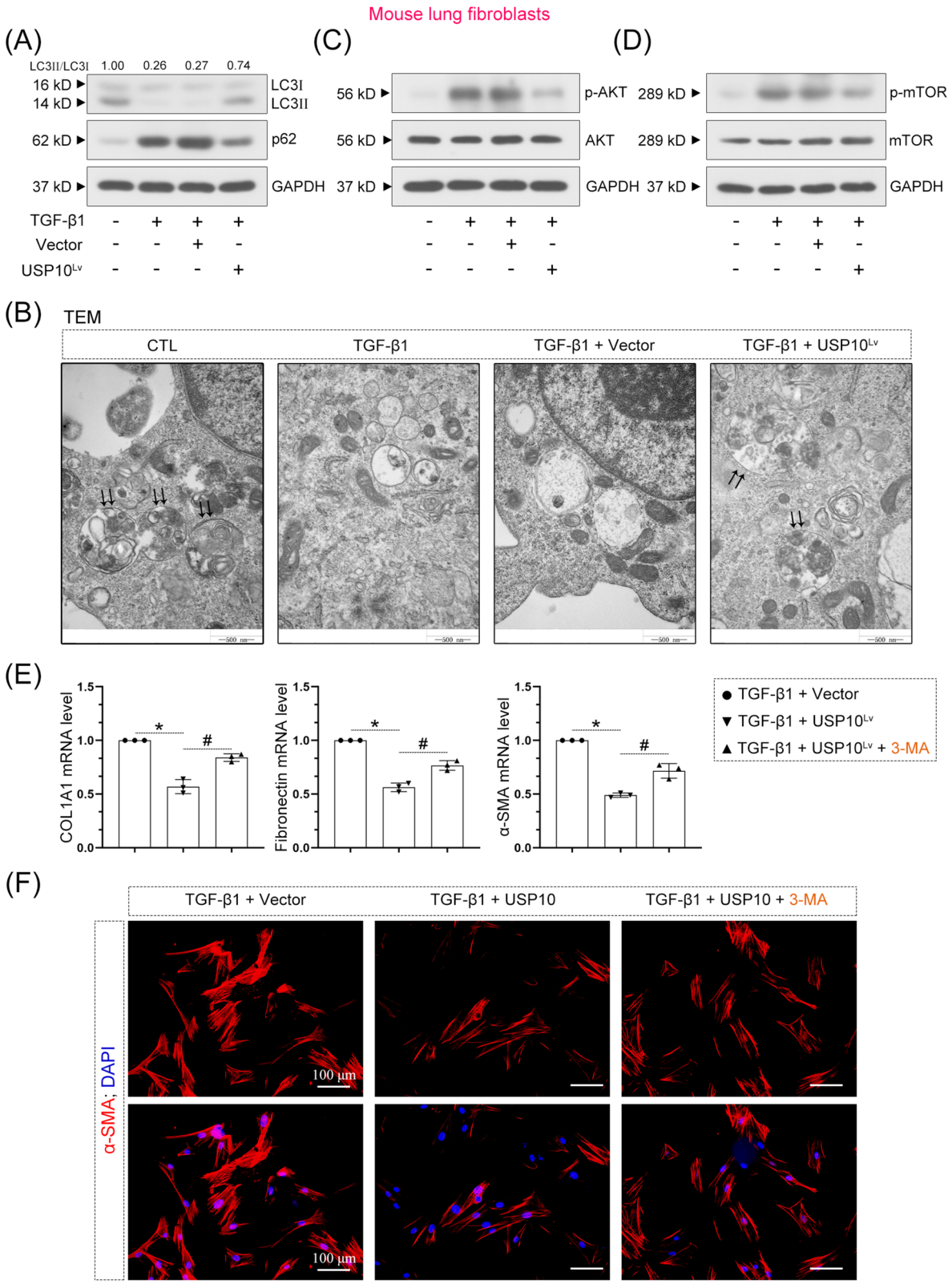
Mouse lung fibroblasts
(A)
LC3II/LC3I 1.00 0.26 0.27 0.74
16 kD
14 kD
LC3I
LC3II
62 kD
p62
37 kD
GAPDH
TGF-β1 - + + +
Vector - - + -
USP10Lv - - - +
(C)
56 kD
p-AKT
56 kD
AKT
37 kD
GAPDH
- + + +
- - + -
- - - +
(D)
289 kD
p-mTOR
289 kD
mTOR
37 kD
GAPDH
- + + +
- - + -
- - - +
(B)
TEM
CTL
TGF-β1
TGF-β1 + Vector
TGF-β1 + USP10Lv
500 nm
(E)
COL1A1 mRNA level
Fibronectin mRNA level
α-SMA mRNA level
1.5
1.0
0.5
0.0
*
#
● TGF-β1 + Vector
▼ TGF-β1 + USP10Lv
▲ TGF-β1 + USP10Lv + 3-MA
(F)
TGF-β1 + Vector
TGF-β1 + USP10
TGF-β1 + USP10 + 3-MA
α-SMA; DAPI
100 μm

◂**Fig. 7** Effect of USP10 on fibrosis and autophagy in TGF-β1-treated mouse lung fibroblasts. **(A)** TGF-β1 treatment resulted in the downregulation of LC3II and upregulation of p62 protein levels. USP10 overexpression reversed the marker of autophagosome expression. **(B)** Representative images of autophagosomes examined using a TEM analysis in MLF. Scale bar = 500 nm. **(C, D)** Western blot results exhibited that p-AKT and p-mTOR were highly upregulated by TGF-β1 treatment. USP10 overexpression inhibited the levels of p-AKT and p-mTOR. **(E)** Fibrotic proteins including COL1 A, fibronectin, and α-SMA increased in the TGF-β1-treated fibroblast following USP10 overexpression. 3-MA treatment reversed fibrotic protein expression. Each bar represents the mean ± SD; $^{*}p < 0.05$ vs. TGF-β1 + Vector group; $^{\#}p < 0.05$ vs. TGF-β1 + $USP10^{Lv}$ group. **(F)** Immunofluorescence staining of α-SMA in TGF-β1-treated mouse lung fibroblast following USP10 overexpression, and 3-MA treatment increased α-SMA expression. USP10, ubiquitin-specific peptidase 10; α-SMA, α-smooth muscle actin; COL1 A, collagen type I alpha1; TEM, transmission electron microscope. MLF, mouse lung fibroblasts

was positively correlated with Sirt6, as evidenced by upregulated Sirt6 expression in USP10-overexpressed HLF (Fig. S1I).

Discussion

Public datasets and results from our findings demonstrated that USP10, a ubiquitin-specific protease, was downregulated in IPF. This study characterized the anti-fibrotic property of USP10 in BLM-induced IPF-like mice and TGF-β1-induced fibroblasts. USP10 overexpression might protect against lung fibrosis by promoting autophagic activity in primary lung fibroblasts through the Sirt6-mediated AKT/mTOR signaling pathway. We explored whether and how USP10 protected against IPF and illustrated the possible mechanisms.

BLM administration induces increased pulmonary inflammation, loss of lung function, and fibrotic changes in the murine lung tissues (Della Latta et al. 2015). Consistent with previously reported findings (Raish et al. 2018), the results showed that BLM administration caused IPF-like phenotypes in mice, as evidenced by obvious histopathological changes, elevated lung index, and collagen deposition. In addition to inducing pathological alterations, BLM also leads to downregulation of pulmonary USP10 expression. Interestingly, the downregulation of USP10 in lung tissues was time-dependent according to the current study from our data and GEO dataset, suggesting that USP10 might be related to IPF development. BLM induction for one week leads to inflammatory responses, and more severe fibrotic scarring and collagen deposition from week 1 through week 3 following BLM induction (Chaudhary et al. 2006; Gupte et al. 2009). Our results indicated that USP10 was downregulated during both the inflammatory and fibrotic phases, and USP10 downregulation was based on a time-dependent manner. More importantly, USP10 was significantly downregulated for three successive weeks, but no longer changed after three weeks in the dataset of GSE37635. We here speculated that BLM injection for three weeks might cause severe fibrosis and three-week treatment was commonly used to induce fibrosis (Izumo et al. 2009; Suzuki et al. 2003). TGF-β1, a major driver of tissue fibrosis, leads to pathological fibrosis by promoting fibroblast infiltration and proliferation, extracellular matrix deposition, and inflammatory responses in almost all contexts (Ren et al. 2023; Saito et al. 2022). In vitro study, we selected TGF-β1-induced primary MLF and HLF to mimic the IPF circumstance.

Impaired autophagy is thought to be a pathogenic driver of IPF (Hosseinzadeh et al. 2018; Patel et al. 2012). As a physiological autophagy inducer, spermidine attenuates BLM-induced lung fibrosis by promoting autophagy (Baek et al. 2020). Autophagy induction by regulation of miR- 33 augments protection against BLM-induced pulmonary fibrosis (Ahangari et al. 2023). In agreement with findings reported by Cabrera et al. (Cabrera et al. 2015), we found BLM administration activated autophagy. However, Baek et al. reported no significant changes in autophagic activity in BLM-induced lung tissues (Baek et al. 2020). Moreover, autophagic activity was suppressed in TGF-β1-treated fibroblast, as previously described (Tsoyi et al. 2021) and in our finding. Interestingly, evidence suggests that USP10 is associated with autophagic activity (Jia and Bonifacino 2021), and USP10 overexpression alleviates chronic liver disease by restoring autophagic activity and promoting autophagic flux (Xin et al. 2023). Indeed, overexpression of USP10 promoted autophagy activation, evidenced by the formation of autophagosomes and expression of key autophagic molecules in BLM-induced fibrotic lung tissue and TGF-β1-induced lung fibroblasts.

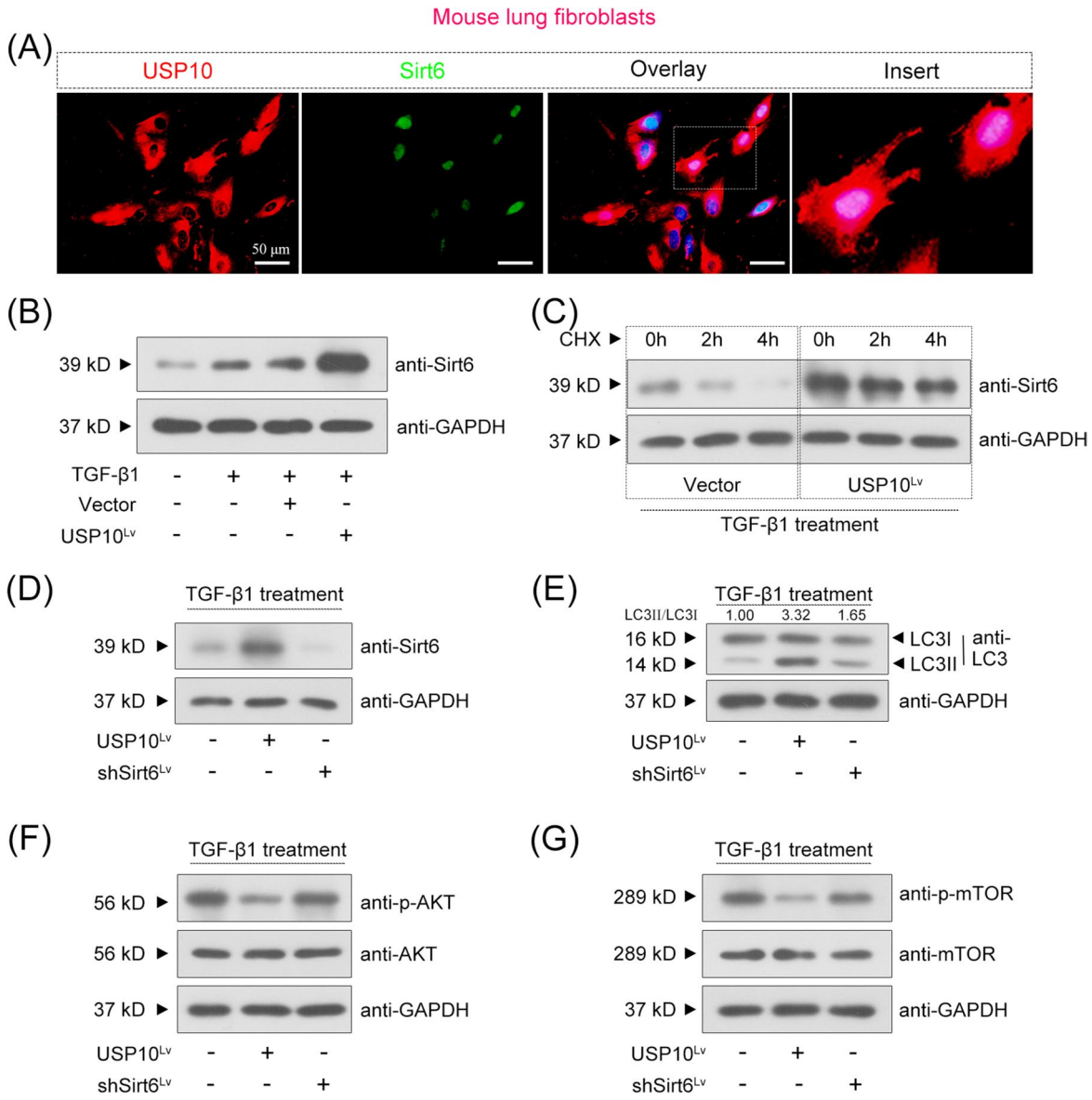

Fig. 8 Effect of USP10 on fibrosis and autophagy depends on Sirt6. **(A)** Representative images of double-labeled immunofluorescence staining of USP10 (red) and Sirt6 (green) in MLF. Blue indicates nucleus marked with DAPI. **(B)** Western blot results showed that Sirt6 expression was increased by TGF-β1 treatment and was further promoted by USP10 overexpression. **(C)** Stability testing uncovered that Sirt6 stability was promoted by USP10 overexpression. Results of Western blot elucidated that USP10 overexpression enhanced the expression of Sirt6 **(D)** and LC3II/LC3I ratio **(E)**, and inhibited p-AKT **(F)** and p-mTOR **(G)** levels. Interference of Sirt6 caused these expression trends to be reversed. USP10, ubiquitin-specific peptidase 10; Sirt6, Sirtuin 6

Mechanically, we revealed that USP10 might alleviate fibrogenesis by modulating the Sirt6-mediated AKT/mTOR pathway, one of the classic autophagy-related pathways (Heras-Sandoval et al. 2014). USP10 regulated the ubiquitination and degradation of downstream proteins (Yuan et al. 2010). Interestingly, USP10 interacted with Sirt6 and mediated its ubiquitination and stabilization (Liu et al. 2022). USP10 was confirmed to co-locate and positively correlated with Sirt6 in lung tissues and fibroblasts.

In addition, USP10 inhibited the activation of AKT/mTOR signaling (Lu et al. 2018). Consistently, the suppression of the AKT/mTOR pathway by USP10 was detected in our study, and these data further confirmed that USP10 promoted autophagy in IPF.

To identify the potential target of IPF, publicly available microarray databases were performed to explore gene expression in IPF. Dataset GSE37635 caught our attention since this dataset compares multiple time points of IPF. USP10 appeared as an appealing candidate following gene ontology analysis, and USP10 was associated with autophagy and cellular response to interleukin-1, which were required for proper lung development. In addition to USP10, some other genes may also be potential targets of IPF, and the role of these factors awaits further investigation. Our current study at least explored the potential role of USP10 in IPF. We are inspired by the public dataset in IPF to screen potential factors. However, we did not perform microarray analysis by ourselves. We will further investigate the role of USP10 in IPF by analyzing our harvested samples. Another limitation of our study was that although we revealed downregulation of USP10 in IPF patients, it was limited by the small number of samples. Thus, we will collect more human lung tissues in future studies to explore USP10 expression and the clinical effects of USP10 on IPF.

Taken together, our results suggest that overexpression of USP10 might attenuate pulmonary fibrogenesis by partially promoting autophagy via the Sirt6-mediated AKT/mTOR pathway. This study will enrich the underlying mechanism of the development of IPF and show that the USP10 supplement could be a novel strategy for lung fibrosis treatment.

Author contribution Shitao Mao participated in the data interpretation and writing the manuscript. Na Yu, Wei Wang, Yikai Mao, and Ying Du carried out the experiments and analyzed data. Shitao Mao, Xiu Gu, Qihe Zhao, and Jian Kang conceived and designed the study, and interpreted the data. All authors read and approved the final paper.

Funding Not applicable.

Data availability No datasets were generated or analysed during the current study.

Declarations

Ethical approval All experimental procedures were approved by the Committee of the Fourth Affiliated Hospital of China Medical University.

Consent for publication Not applicable.

Conflicts of interest The authors declare no competing interests.

References

Ahangari F, Price NL, Malik S, Chioccioli M, Bärnthaler T, Adams TS, et al. microRNA-33 deficiency in macrophages enhances autophagy, improves mitochondrial homeostasis, and protects against lung fibrosis. JCI insight. 2023;8:e158100.

Araya J, Hara H, Kuwano K. Autophagy in the pathogenesis of pulmonary disease. Intern Med. 2013a;52:2295–303.

Araya J, Kojima J, Takasaka N, Ito S, Fujii S, Hara H, et al. Insufficient autophagy in idiopathic pulmonary fibrosis. Am J Physiol Lung Cell Mol Physiol. 2013b;304:L56–69.

Baek AR, Hong J, Song KS, Jang AS, Kim DJ, Chin SS, et al. Spermidine attenuates bleomycin-induced lung fibrosis by inducing autophagy and inhibiting endoplasmic reticulum stress (ERS)-induced cell death in mice. Exp Mol Med. 2020;52:2034–45.

Blaauboer ME, Emson CL, Verschuren L, van Erk M, Turner SM, Everts V, et al. Novel combination of collagen dynamics analysis and transcriptional profiling reveals fibrosis-relevant genes and pathways. Matrix Biol. 2013;32:424–31.

Cabrera S, Maciel M, Herrera I, Nava T, Vergara F, Gaxiola M, et al. Essential role for the ATG4B protease and autophagy in bleomycin-induced pulmonary fibrosis. Autophagy. 2015;11:670–84.

Chaudhary NI, Schnapp A, Park JE. Pharmacologic differentiation of inflammation and fibrosis in the rat bleomycin model. Am J Respir Crit Care Med. 2006;173:769–76.

Chen J, Xie J-J, Jin M-Y, Gu Y-T, Wu C-C, Guo W-J, et al. Sirt6 overexpression suppresses senescence and apoptosis of nucleus pulposus cells by inducing autophagy in a model of intervertebral disc degeneration. Cell Death Dis. 2018;9:56.

Della Latta V, Cecchettini A, Del Ry S, Morales MA. Bleomycin in the setting of lung fibrosis induction: From biological mechanisms to counteractions. Pharmacol Res. 2015;97:122–30.

Gao F, Qian M, Liu G, Ao W, Dai D, Yin C. USP10 alleviates sepsis-induced acute kidney injury by regulating Sirt6-mediated Nrf2/ARE signaling pathway. J Inflamm (Lond). 2021;18:25.

Gupte VV, Ramasamy SK, Reddy R, Lee J, Weinreb PH, Violette SM, et al. Overexpression of fibroblast growth factor-10 during both inflammatory and fibrotic phases attenuates bleomycin-induced pulmonary fibrosis in mice. Am J Respir Crit Care Med. 2009;180:424–36.

Heras-Sandoval D, Pérez-Rojas JM, Hernández-Damián J, Pedraza-Chaverri J. The role of PI3K/AKT/mTOR pathway in the modulation of autophagy and the clearance of protein aggregates in neurodegeneration. Cell Signal. 2014;26:2694–701.

Hill C, Li J, Liu D, Conforti F, Brereton CJ, Yao L, et al. Autophagy inhibition-mediated epithelial-mesenchymal transition augments local myofibroblast differentiation in pulmonary fibrosis. Cell Death Dis. 2019;10:591.

Hosseinzadeh A, Javad-Moosavi SA, Reiter RJ, Yarahmadi R, Ghaznavi H, Mehrzadi S. Oxidative/nitrosative stress, autophagy and apoptosis as therapeutic targets of melatonin in idiopathic pulmonary fibrosis. Expert Opin Ther Targets. 2018;22:1049–61.

Izumo T, Kondo M, Nagai A. Effects of a leukotriene B4 receptor antagonist on bleomycin-induced pulmonary fibrosis. Eur Respir J. 2009;34:1444–51.

Jia R, Bonifacino JS. The ubiquitin isopeptidase USP10 deubiquitinates LC3B to increase LC3B levels and autophagic activity. J Biol Chem. 2021;296:100405.

Levine B, Kroemer G. Autophagy in the pathogenesis of disease. Cell. 2008;132:27–42.

Li J, Li P, Zhang G, Qin P, Zhang D, Zhao W. CircRNA TADA2A relieves idiopathic pulmonary fibrosis by inhibiting proliferation and activation of fibroblasts. Cell Death Dis. 2020a;11:553.

Li Y, Liu R, Wu J, Li X. Self-eating: friend or foe? The emerging role of autophagy in fibrotic diseases. Theranostics. 2020b;10:7993–8017.

Liu M, Liang K, Zhen J, Zhou M, Wang X, Wang Z, et al. Sirt6 deficiency exacerbates podocyte injury and proteinuria through targeting Notch signaling. Nat Commun. 2017;8:413.

Liu LB, Huang SH, Qiu HL, Cen XF, Guo YY, Li D, et al. Limonin stabilises sirtuin 6 (SIRT6) by activating ubiquitin specific peptidase 10 (USP10) in cardiac hypertrophy. Br J Pharmacol. 2022;179:4516–33.

Lu C, Ning Z, Wang A, Chen D, Liu X, Xia T, et al. USP10 suppresses tumor progression by inhibiting mTOR activation in hepatocellular carcinoma. Cancer Lett. 2018;436:139–48.

Lu L, Ma J, Liu Y, Shao Y, Xiong X, Duan W, et al. FSTL1-USP10-Notch1 signaling axis protects against cardiac dysfunction through inhibition of myocardial fibrosis in diabetic mice. Front Cell Dev Biol. 2021;9:757068.

Luo P, Qin C, Zhu L, Fang C, Zhang Y, Zhang H, et al. Ubiquitin-Specific Peptidase 10 (USP10) inhibits hepatic steatosis, insulin resistance, and inflammation through Sirt6. Hepatology. 2018;68:1786–803.

Nakahira K, PabonPorras MA, Choi AMK. Autophagy in pulmonary diseases. Am J Respir Crit Care Med. 2016;194:1196–207.

Neel BA, Lin Y, Pessin JE. Skeletal muscle autophagy: a new metabolic regulator. Trends Endocrinol Metab. 2013;24:635–43.

Patel AS, Lin L, Geyer A, Haspel JA, An CH, Cao J, et al. Autophagy in idiopathic pulmonary fibrosis. PLoS ONE. 2012;7:e41394.

Raish M, Ahmad A, Ahmad Ansari M, Ahad A, Al-Jenoobi FI, Al-Mohizea AM, et al. Sinapic acid ameliorates bleomycin-induced lung fibrosis in rats. Biomed Pharmacother. 2018;108:224–31.

Ren LL, Li XJ, Duan TT, Li ZH, Yang JZ, Zhang YM, et al. Transforming growth factor-β signaling: From tissue fibrosis to therapeutic opportunities. Chem Biol Interact. 2023;369:110289.

Richeldi L, Costabel U, Selman M, Kim DS, Hansell DM, Nicholson AG, et al. Efficacy of a tyrosine kinase inhibitor in idiopathic pulmonary fibrosis. N Engl J Med. 2011;365:1079–87.

Richeldi L, du Bois RM, Raghu G, Azuma A, Brown KK, Costabel U, et al. Efficacy and safety of nintedanib in idiopathic pulmonary fibrosis. N Engl J Med. 2014;370:2071–82.

Richeldi L, Collard HR, Jones MG. Idiopathic pulmonary fibrosis. Lancet. 2017;389:1941–52.

Ryter SW, Nakahira K, Haspel JA, Choi AMK. Autophagy in pulmonary diseases. Annu Rev Physiol. 2012;74:377–401.

Saito S, Deskin B, Rehan M, Yadav S, Matsunaga Y, Lasky JA, et al. Novel mediators of idiopathic pulmonary fibrosis. Clin Sci (Lond). 2022;136:1229–40.

Sgalla G, Iovene B, Calvello M, Ori M, Varone F, Richeldi L. Idiopathic pulmonary fibrosis: pathogenesis and management. Respir Res. 2018;19:32.

Singh KK, Lovren F, Pan Y, Quan A, Ramadan A, Matkar PN, et al. The essential autophagy gene ATG7 modulates organ fibrosis via regulation of endothelial-to-mesenchymal transition. J Biol Chem. 2015;290:2547–59.

Suzuki H, Aoshiba K, Yokohori N, Nagai A. Epidermal growth factor receptor tyrosine kinase inhibition augments a murine model of pulmonary fibrosis. Cancer Res. 2003;63:5054–9.

Takahashi M, Higuchi M, Makokha GN, Matsuki H, Yoshita M, Tanaka Y, et al. HTLV-1 Tax oncoprotein stimulates ROS production and apoptosis in T cells by interacting with USP10. Blood. 2013a;122:715–25.

Takahashi M, Higuchi M, Matsuki H, Yoshita M, Ohsawa T, Oie M, et al. Stress granules inhibit apoptosis by reducing reactive oxygen species production. Mol Cell Biol. 2013b;33:815–29.

Tian K, Chen P, Liu Z, Si S, Zhang Q, Mou Y, et al. Sirtuin 6 inhibits epithelial to mesenchymal transition during idiopathic pulmonary fibrosis via inactivating TGF-β1/Smad3 signaling. Oncotarget. 2017;8:61011–24.

Tsoyi K, Liang X, De Rossi G, Ryter SW, Xiong K, Chu SG, et al. CD148 deficiency in fibroblasts promotes the development of pulmonary fibrosis. Am J Respir Crit Care Med. 2021;204:312–25.

Wang X, Xia S, Li H, Wang X, Li C, Chao Y, et al. The deubiquitinase USP10 regulates KLF4 stability and suppresses lung tumorigenesis. Cell Death Differ. 2020;27:1747–64.

Xin SL, Pan XL, Xu XY, Yu YY. USP10 Alleviates palmitic acid-induced steatosis through autophagy in HepG2 Cells. J Clin Transl Hepatol. 2023;11:45–57.

Yuan J, Luo K, Zhang L, Cheville JC, Lou Z. USP10 regulates p53 localization and stability by deubiquitinating p53. Cell. 2010;140:384–96.

Zhang D-H, Zhang J-L, Huang Z, Wu L-M, Wang Z-M, Li Y-P, et al. Deubiquitinase ubiquitin-specific protease 10 deficiency regulates sirt6 signaling and exacerbates cardiac hypertrophy. J Am Heart Assoc. 2020;9:e017751.

Zhang Q, Tu W, Tian K, Han L, Wang Q, Chen P, et al. Sirtuin 6 inhibits myofibroblast differentiation via inactivating transforming growth factor-β1/Smad2 and nuclear factor-κB signaling pathways in human fetal lung fibroblasts. J Cell Biochem. 2019;120:93–104.